

Supplementary Materials for CryoEM structure of MxB reveals a novel oligomerization interface critical for HIV restriction

Frances J. D. Alvarez, Shaoda He, Juan R. Perilla, Sooin Jang, Klaus Schulten, Alan N. Engelman,
Sjors H. W. Scheres, Peijun Zhang

Published 15 September 2017, *Sci. Adv.* **3**, e1701264 (2017)
DOI: 10.1126/sciadv.1701264

The PDF file includes:

- table S1. Effects of MxB mutations at intermolecular interfaces 1, 3, and 4.
- fig. S1. Sequence alignment of Mx and dynamin proteins.
- fig. S2. MxB assembles into helical tubes with and without the MBP tag.
- fig. S3. GTPase activity of MBP-MxB at different protein and salt concentrations.
- fig. S4. MBP-MxB tubes in the presence of GTP without or with MgCl₂.
- fig. S5. CryoEM of the MBP-MxB assembly.
- fig. S6. Handedness of the MxB helical assembly map.
- fig. S7. Gold-standard Fourier shell correlation curve of the MBP-MxB density map.
- fig. S8. MDFF and real-space refinement of the MxB helical assembly model.
- fig. S9. Enlarged views of the intermolecular interfaces in the MxB assembly.
- fig. S10. Comparison of interfaces between cryoEM and crystal structures.
- fig. S11. Comparison of L1 and L2 contacts of MxB and dynamin 3.
- fig. S12. Interface 4 mutations relative to GTP-binding site.
- fig. S13. Comparison of MxB and MxA GTPase-BSE domains.

Other Supplementary Material for this manuscript includes the following: (available at advances.sciencemag.org/cgi/content/full/3/9/e1701264/DC1)

- movie S1 (.mp4 format). Molecular dynamics flexible fitting of MxB into the cryoEM map.
- movie S2 (.mp4 format). MxB assembles into a helical array.
- movie S3 (.mp4 format). α 1c helix kinks from linear to tubular array.
- movie S4 (.mp4 format). Formation of Interface 3 during helical assembly.

table S1. Effects of MxB mutations at intermolecular interfaces 1, 3, and 4.

Interface	Mutation	Fold Effect on HIV-1 restriction*	Oligomerization [#]	References
Putative Interface 1 crystal	I423D	< 1 ×	ND	(15)
		ND	>250kDa ^{xl}	(19)
		~ 1 ×	>250kDa ^{xl}	(18)
	E424R	~ 1 ×	>250kDa ^{xl}	(19)
	K663D	< 1 ×	ND	(15)
		~ 0.8	>250kDa ^{xl}	(19)
	M666D	< 1 ×	ND	(15)
		ND	>250kDa ^{xl}	(19)
		< 1 ×	>250kDa ^{xl}	(18)
L669D	~ 2 ×	>250kDa ^{xl}	(19)	
I423D/K663D	~ 1 ×	dimer ^{gf}	(15)	
I423D/K663D/M666D	ND	dimer ^{gf}		
Interface 1 cryoEM	F420D	~ 1 ×	oligomers ^{em}	This study
	K693D	~ 1 ×	ND	
	F420D/K693D	~ 1 ×	ND	
Interface 3 cryoEM	E484K	~ 3 ×	ND	This study
	F495D	~ 3.5 ×	No oligomers ^{em}	
	R449D	~ 3 ×	No oligomers ^{em}	
Interface 4 cryoEM	E285K	~ 1 ×	oligomers ^{em}	This study
	W677D	~ 1 ×	ND	
	E285K/W677D	~ 1 ×	ND	
Other mutations	Δ440-448(L1)/GSGGSG	~ 2 ×	ND	(11)
	Δ488-497(L2)/GSGGSG	~ 3.5 ×	ND	
	Δ584-615(L4)/GAGAG	~ 2 ×	ND	
	Δ580-608 (L4)	~ 2 ×	~ 190kDa ^{xl}	(18)
	G439D	~ 1 ×	ND	(11)
		~ 1 ×	>250kDa ^{xl}	(18) [†]
	R455A	~ 2 ×	ND	(11)
	R455D	~ 5.5 ×	ND	(18) [†]
		~ 5 ×	No oligomers ^{xl}	
	⁴⁸⁷ YRGK ⁴⁹⁰ /AAAA	< 1 ×	~ 190kDa ^{xl}	(15)
		~ 2 ×	ND	
	E681A	~ 1 ×	ND	(18)
~ 2 ×		>250kDa ^{xl}		
R689A	~ 2 ×	ND	(15)	
	~ 2 ×	>250kDa ^{xl}	(18)	

*Fold defect in HIV-1 restriction compared to the wild-type. 2x effect means 50% of wild-type antiviral activity. [#]Measurement of oligomerization by cross-linking (xl) or gel filtration (gf) or electron microscopy (em). [†]Mutations were thought to be at the hypothetical “Interface 3” (18) (fig. S8B). Mutations in bold are from this study and those in red have significantly reduced effect on anti-HIV-1 activity of MxB (cut off at < 3 fold effective compared to the wild-type). ND, not determined.

N-terminal Region (NTR)

MX2_HUMAN 1 MSKAHKWPYRRRSQFSRRKYLKEMNSFQQQPPFPFGTVPPQMMFFPNWQGAEKDAFLAKDFNFLTNNQPPFGNRSQPRAMGPENNL
 MX1_HUMAN 1MNVSEVDIAKADPAASHPELLNGDATVAQKNPGSVAENNL
 MX1_MOUSE 1MDSVNNL
 MX2_MOUSE 1MVLSTEENTGVDSVNLPSGETGLGEKQDESNNL
 MX2_PIG 1 MPKPRMSWPYQRHRQASPPFPHKEMNFFPQPLPLGAGPGQMTFFLNWQMGKDLTKRLNMLTSLPQQPGGKSGQQT5KGPENNL
 MX_CHICKEN 1MNNPWSNFSSAFGCPILQIPKQNSNVPPSLPVPVGVFVPLRSGCSNQMAFCAPELTDKRPPEHEQKVSRLNDREDDKDEAAACSL
 MXA_ZEBRAFISH 1MEKLSYTF
 DYN1_HUMAN 1MG
 DYN2_HUMAN 1MG
 DYN3-2_HUMAN 1MG
 DNM1L_HUMAN 1MG
 DNM1_YEAST 1



MX2_HUMAN 90 YSQYEQKVRPQIDIDSLRALGVQDQLALPATAVIGDQSSGKSSVLEALSGVA.LPRGSGIVTRCPVLVNLKKKOP.....
 MX1_HUMAN 42 CSQYEEKVRPQIDIDSLRALGVQDQLALPATAVIGDQSSGKSSVLEALSGVA.LPRGSGIVTRCPVLVNLKKLVN.....
 MX1_MOUSE 8 CRHYEEKVRPQIDIDSLRALGVQDQLALPATAVIGDQSSGKSSVLEALSGVA.LPRGSGIVTRCPVLVNLKKLKE.....
 MX2_MOUSE 35 CSQYEEKVRPQIDIDSLRALGVQDQLALPATAVIGDQSSGKSSVLEALSGVA.LPRGSGIVTRCPVLVNLKKLNE.....
 MX2_PIG 87 YSPFEERVRPQIDIDSLRALGVQDQLALPATAVIGDQSSGKSSVLEALSGVP.LPRGSGITTRCPVLLVNLKKKE.....
 MX_CHICKEN 96 DNGVRRKROPIDIDSLRALGVQDQLALPATAVIGDQSSGKSSVLEALSGVA.LPRGSGIVTRCPVLLVNLKKMTA.....
 MXA_ZEBRAFISH 9 SQYEEKVRPQIDIDSLRALGVQDQLALPATAVIGDQSSGKSSVLEALSGVP.LPRGSGIVTRCPVLLVNLKKMTA.....
 DYN1_HUMAN 3 NRGMEELPPLVNRQDFFSALGQSCILDLPLAVVGGQSSGKSSVLEALSGVP.LPRGSGIVTRCPVLLVNLKKVAT.....
 DYN2_HUMAN 3 NRGMEELPPLVNRQDFFSALGQSCILDLPLAVVGGQSSGKSSVLEALSGVP.LPRGSGIVTRCPVLLVNLKKVAT.....
 DYN3-2_HUMAN 3 NRGMEELPPLVNRQDFFSALGQSCILDLPLAVVGGQSSGKSSVLEALSGVP.LPRGSGIVTRCPVLLVNLKKVAT.....
 DNM1L_HUMAN 1 ..MEALPPLVNRQDFFSALGQSCILDLPLAVVGGQSSGKSSVLEALSGVP.LPRGSGIVTRCPVLLVNLKKVAT.....
 DNM1_YEAST 1 MASLEDLPLVNRQDFFSALGQSCILDLPLAVVGGQSSGKSSVLEALSGVP.LPRGSGIVTRCPVLLVNLKKVAT.....



MX2_HUMAN 164CEAFAAGRTISVNRTELELDQDGGVEKEIHKANVMAGNGRGISHELISLITSPSPVDDLTIID
 MX1_HUMAN 117EDKWRGVSVQDYEIIISDASEVEKEINKANAGAGEGMIISHELITLISSRDVPDILTID
 MX1_MOUSE 83GEEWRGVSVQDYEIIISDASEVEKEINKANAGAGEGMIISHELITLISSRDVPDILTID
 MX2_MOUSE 110GEEWRGVSVQDYEIIISDASEVEKEINKANAGAGEGMIISHELITLISSRDVPDILTID
 MX2_PIG 161CPWGRGRTISVNRTELELDQDGGVEKEIHKANVMAGNGRGISHELISLITSPSPVDDLTIID
 MX_CHICKEN 161PEWRGVSVQDYEIIISDASEVEKEINKANAGAGEGMIISHELITLISSRDVPDILTID
 MXA_ZEBRAFISH 84QDRHGRVSVQDYEIIISDASEVEKEINKANAGAGEGMIISHELITLISSRDVPDILTID
 DYN1_HUMAN 78TEHAERLHCKG..KRFDFEDEVRELEAEADRVIGNKKGISPVINLVVYSPHVLNLTLDV
 DYN2_HUMAN 78TEHAERLHCKG..KRFDFEDEVRELEAEADRVIGNKKGISPVINLVVYSPHVLNLTLDV
 DYN3-2_HUMAN 78TEHAERLHCKG..KRFDFEDEVRELEAEADRVIGNKKGISPVINLVVYSPHVLNLTLDV
 DNM1L_HUMAN 86 E.....AEWGRVSVQDYEIIISDASEVEKEINKANAGAGEGMIISHELITLISSRDVPDILTID
 DNM1_YEAST 89 PHDEVTKISGFEAGTKPLEYRGKERNHADEWGERLHFGP..KRFDFEDEVRELEAEADRVIGNKKGISPVINLVVYSPHVLNLTLDV



MX2_HUMAN 226 LPGAIRRVAVGNOPADIGRQIKRIRKTYIQKQETINLVVSPNVDIATTEALSMAGVEVDPGDRRTIGILTRKDLMDRGTEKSVMNIVVRNL
 MX1_HUMAN 179 LPGAIRRVAVGNOPADIGRQIKRIRKTYIQKQETINLVVSPNVDIATTEALSMAGVEVDPGDRRTIGILTRKDLMDRGTEKSVMNIVVRNL
 MX1_MOUSE 145 LPGAIRRVAVGNOPADIGRQIKRIRKTYIQKQETINLVVSPNVDIATTEALSMAGVEVDPGDRRTIGILTRKDLMDRGTEKSVMNIVVRNL
 MX2_MOUSE 172 LPGAIRRVAVGNOPADIGRQIKRIRKTYIQKQETINLVVSPNVDIATTEALSMAGVEVDPGDRRTIGILTRKDLMDRGTEKSVMNIVVRNL
 MX2_PIG 222 LPGAIRRVAVGNOPADIGRQIKRIRKTYIQKQETINLVVSPNVDIATTEALSMAGVEVDPGDRRTIGILTRKDLMDRGTEKSVMNIVVRNL
 MX_CHICKEN 223 LPGAIRRVAVGNOPADIGRQIKRIRKTYIQKQETINLVVSPNVDIATTEALSMAGVEVDPGDRRTIGILTRKDLMDRGTEKSVMNIVVRNL
 MXA_ZEBRAFISH 146 LPGAIRRVAVGNOPADIGRQIKRIRKTYIQKQETINLVVSPNVDIATTEALSMAGVEVDPGDRRTIGILTRKDLMDRGTEKSVMNIVVRNL
 DYN1_HUMAN 137 LPGAIRRVAVGNOPADIGRQIKRIRKTYIQKQETINLVVSPNVDIATTEALSMAGVEVDPGDRRTIGILTRKDLMDRGTEKSVMNIVVRNL
 DYN2_HUMAN 137 LPGAIRRVAVGNOPADIGRQIKRIRKTYIQKQETINLVVSPNVDIATTEALSMAGVEVDPGDRRTIGILTRKDLMDRGTEKSVMNIVVRNL
 DYN3-2_HUMAN 137 LPGAIRRVAVGNOPADIGRQIKRIRKTYIQKQETINLVVSPNVDIATTEALSMAGVEVDPGDRRTIGILTRKDLMDRGTEKSVMNIVVRNL
 DNM1L_HUMAN 147 LPGAIRRVAVGNOPADIGRQIKRIRKTYIQKQETINLVVSPNVDIATTEALSMAGVEVDPGDRRTIGILTRKDLMDRGTEKSVMNIVVRNL
 DNM1_YEAST 176 LPGAIRRVAVGNOPADIGRQIKRIRKTYIQKQETINLVVSPNVDIATTEALSMAGVEVDPGDRRTIGILTRKDLMDRGTEKSVMNIVVRNL



MX2_HUMAN 315 VYPLKKGVMVVKCRGQDEITNRLSLAEATKKEIHFQTHPVFRVLLREGSATVPLAERLLEITIMHTQKSLPDLLEGOVRESHQHATE
 MX1_HUMAN 268 VYHLKKGVMVVKCRGQDEIQDQLSLEALQREKIFFENHPVFRDLEEGKATVPLAERLLEITIMHTQKSLPDLLENOKETHQHATE
 MX1_MOUSE 234 VYPLKKGVMVVKCRGQDEIQDQLSLEALQREKIFFENHPVFRDLEEGKATVPLAERLLEITIMHTQKSLPDLLENOKETHQHATE
 MX2_MOUSE 261 VYHLKKGVMVVKCRGQDEIQDQLSLEALQREKIFFENHPVFRDLEEGKATVPLAERLLEITIMHTQKSLPDLLENOKETHQHATE
 MX2_PIG 311 VYHLKKGVMVVKCRGQDEINLKLSLAEATKKEIHFQTHPVFRVLLREGSATVPLAERLLEITIMHTQKSLPDLLENOKETHQHATE
 MX_CHICKEN 312 VYPLKKGVMVVKCRGQDEINLKLSLAEATKKEIHFQTHPVFRVLLREGSATVPLAERLLEITIMHTQKSLPDLLENOKETHQHATE
 MXA_ZEBRAFISH 235 VYHLKKGVMVVKCRGQDEIMDQVTLNEAEESAFKDHHPVFRDLEEGKATVPLAERLLEITIMHTQKSLPDLLENOKETHQHATE
 DYN1_HUMAN 224 LPLLRRCYIGVVRNSQDDIGKDDIATAAARERFFLSHPAYRHLAD..RMGTPPLQKVLNQQTNIHRSBLSBALRSKQSOQLLSEIE
 DYN2_HUMAN 224 LPLLRRCYIGVVRNSQDDIGKDDIATAAARERFFLSHPAYRHLAD..RMGTPPLQKVLNQQTNIHRSBLSBALRSKQSOQLLSEIE
 DYN3-2_HUMAN 224 LPLLRRCYIGVVRNSQDDIGKDDIATAAARERFFLSHPAYRHLAD..RMGTPPLQKVLNQQTNIHRSBLSBALRSKQSOQLLSEIE
 DNM1L_HUMAN 234 VYPLKKGVMVVKCRGQDEINLKLSLAEATKKEIHFQTHPVFRVLLREGSATVPLAERLLEITIMHTQKSLPDLLENOKETHQHATE
 DNM1_YEAST 263 MYPLRLRGLVGVVRNSQDDIQLNKTVESLDRBEDYFRKHEVYRTIST..KCGTRYLARLNLQTLNLSHIRDKLDDIKRNLNLTISQTECE

Figure S1 continue



fig. S1. Sequence alignment of Mx and dynamin proteins. Amino acid sequences of Mx and dynamin proteins were aligned using MUSCLE and the alignment visualized using ESPrnt3. The sequences include: MX2_HUMAN (Uniprot ID P20592), MX1_HUMAN (P20591), MX1_MOUSE (P09922), MX2_MOUSE (Q9WVP9), MX2_PIG (A7VK00), MX_CHICKEN (Q90597), MXA_ZEBRAFISH (Q8JH68), DYN1_HUMAN (Q05193), DYN2_HUMAN (P50570), DYN3-3_HUMAN (Q9UQ16), DNMI1L_HUMAN (O00429) and DNMI1_YEAST (P54861). Residues with a conservation of greater than 70% are color-coded (D, E in red; R, K, H in blue; N, Q, S, T in grey; L, I, V, F, Y, W, M, C in green; P, G in brown). Alpha-helices are shown as cylinders, while beta-sheets as arrows, with colors as in Figure 3C. The N-terminal region is represented as red dashed line and the unresolved regions in black dashed line. Residues involved in the interfaces (1, 3 and 4) are indicated on top of the alignment in bold (black in this study, red for MxB crystal contacts, 4WHJ) or at the bottom underlined (for dynamin 3 tetramer, 5A3F) and italicized (for MxA crystal contacts, 3SZR).

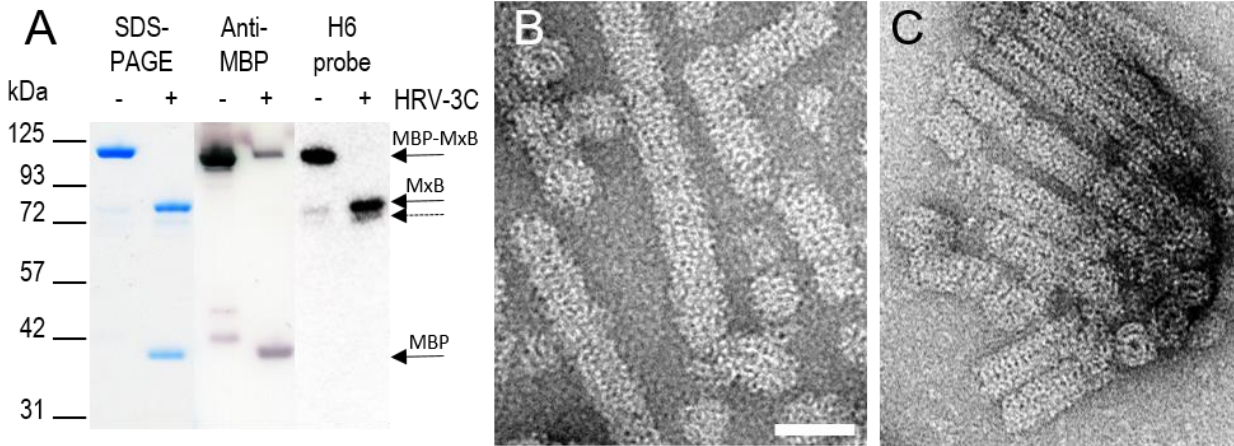


fig. S2. MxB assembles into helical tubes with and without the MBP tag. (A) Coomassie-stained SDS-PAGE gel and corresponding western blots, with the indicated primary antibody or probe. MBP-MxB-H6 was treated as indicated with HRV-3C protease at 150 mM NaCl. Proteins are indicated by arrows on the right. Dashed arrow points to a minor species of MxB with both MBP and the linker between MBP and MxB removed. (B&C) Negative stain EM images of samples in (A) without the protease (B) and with the protease (C). Removal of the MBP-tag resulted in ordered, but largely aggregated, MxB tubes. Scale bar, 50 nm.

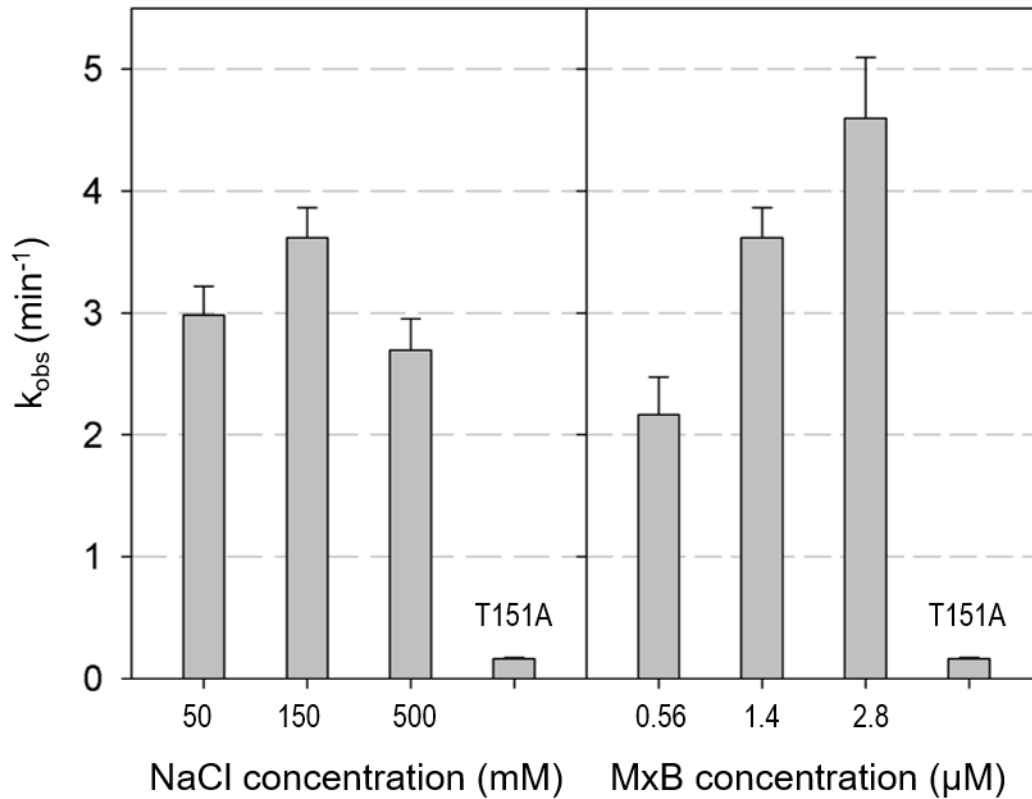


fig. S3. GTPase activity of MBP-MxB at different protein and salt concentrations.

GTPase activities on the left were measured at a constant MxB concentration of 1.4 μM, and on the right were measured at a constant NaCl concentration of 150 mM. GTPase activities of wt MxB were assayed using a continuous NADH-coupled assay at 1 mM GTP and 37°C. Each gray bar represents the mean of three independent measurements while the error bars represent the 95% confidence interval. MxB T151A at 1.3 μM concentration and 150 mM NaCl is included as negative control.

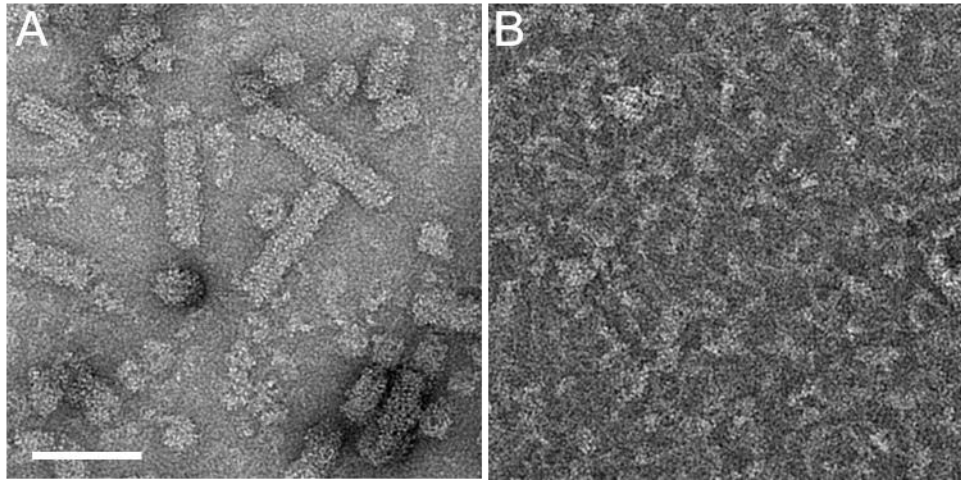


fig. S4. MBP-MxB tubes in the presence of GTP without or with MgCl₂. Negative-stain projection image of MBP-MxB helical assembly after incubating with assembly buffer for 2 hours in the presence of GTP without (**A**) and with MgCl₂ (**B**). Scale bar, 100 nm.

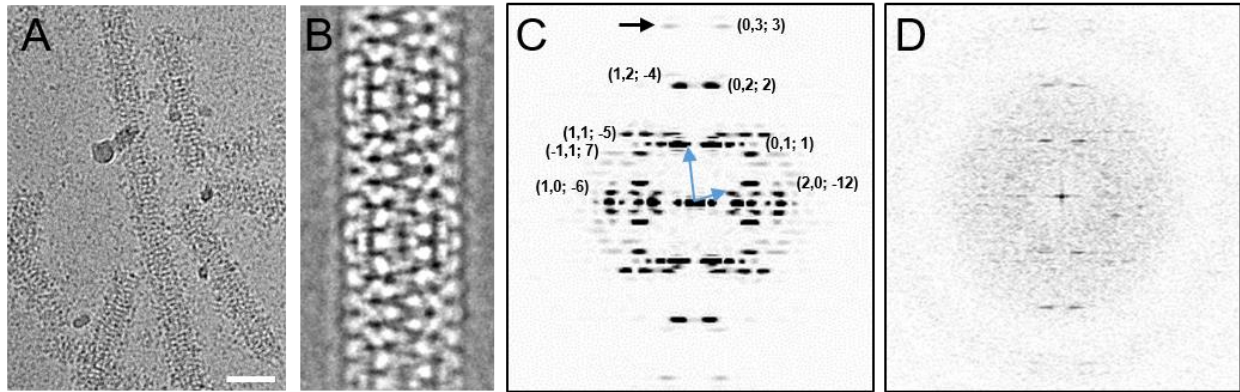


fig. S5. CryoEM of the MBP-MxB assembly. (A) A low-dose projection image of MBP-MxB tubular assembly. Scale bar, 50 nm. (B) A 2D class average of MxB tubes. (C) Fourier transform of the class average in B. The tube belongs to a 1-start helical family of $(-6, 1)$. Helical indices are shown. Blue arrows point to the two vectors $(1,0; -6)$ and $(0,1; 1)$ in helical indexing. Black arrow points to the layer-line at 16 \AA resolution. (D) A Fourier transform of a raw image of MBP-MxB tube.

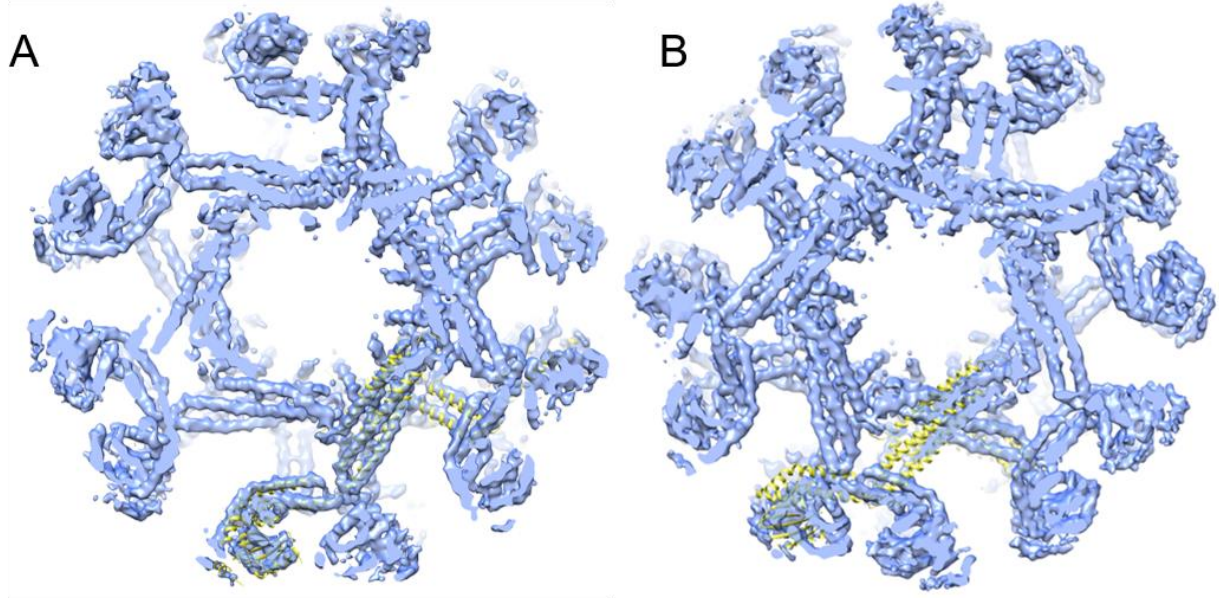


fig. S6. Handedness of the MxB helical assembly map. (A) Docking of the crystal structure of dimer MxB (PDB:4WHJ, yellow) into the right-handed MBP-MxB helical assembly map. (B) Docking of the crystal structure of dimer MxB into the left-handed map.

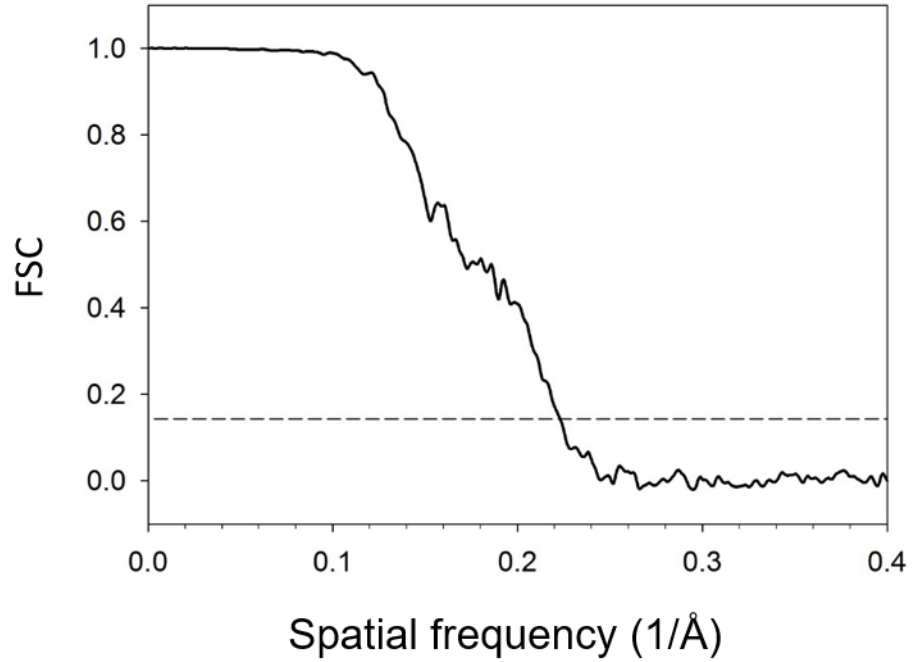


fig. S7. Gold-standard Fourier shell correlation curve of the MBP-MxB density map. The overall resolution is 4.6 Å using an FSC cut-off of 0.143.

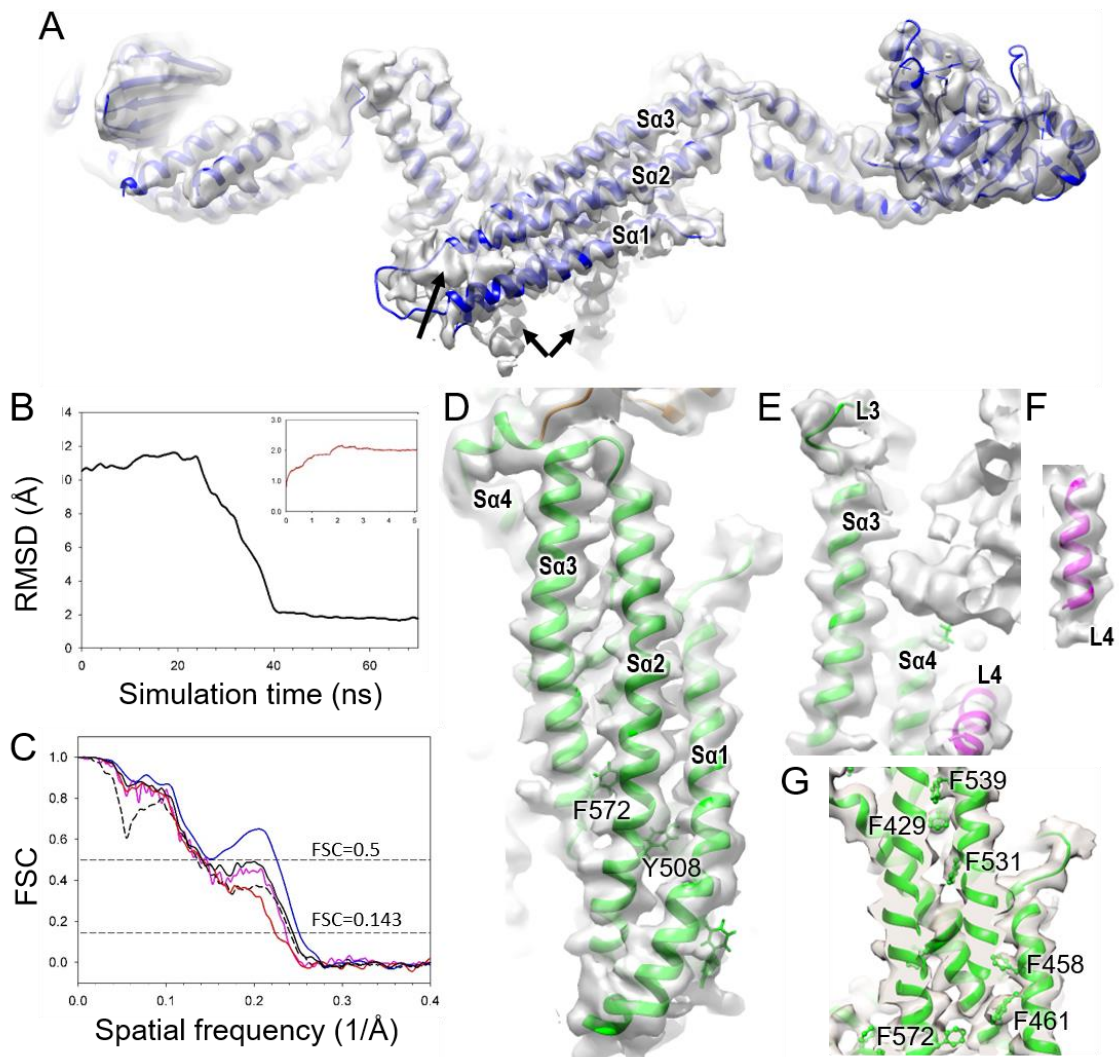


fig. S8. MDFF and real-space refinement of the MxB helical assembly model. (A) Rigid body docking of individual domains of the MxB crystal structure (4WHJ). Arrows point to densities that do not fit. (B) Time-evolution of the $C\alpha$ -RMSD between the MDFF simulation and the initial MxB dimer model; the initial model was built based on the MxB crystal-structure. Inset: time-evolution of the $C\alpha$ -RMSD for the refinement of the MDFF-derived tubular model; the MDFF model is refined by applying a series of gaussian-smoothed electron-densities with sigma decreasing from 5 to 0 Å in 1 Å steps. Note the difference in the scale. (C) FSC curves between the cryo-EM density map and the molecular models of MxB GTPase-BSE domain (red), Stalk domain (blue), dimer (black), tube (purple), and rigid body docking of individual domains of the crystal structure (dashed black). (D to F) Representative views of the fitting of the refined model into the density map: stalk helices (Sa1, Sa2 and Sa3, along with bulky amino acids Y508 and F572) (D), stalk helices (Sa3 and Sa4) and loops (L3, L4 helix) (E), and clear helical density in L4 (F). The extra unfitted density in (E) is from the other monomer.

(G) A clipped view shows densities of bulky amino acid side chains (F539, F429, F531, F458, F461 and F572).

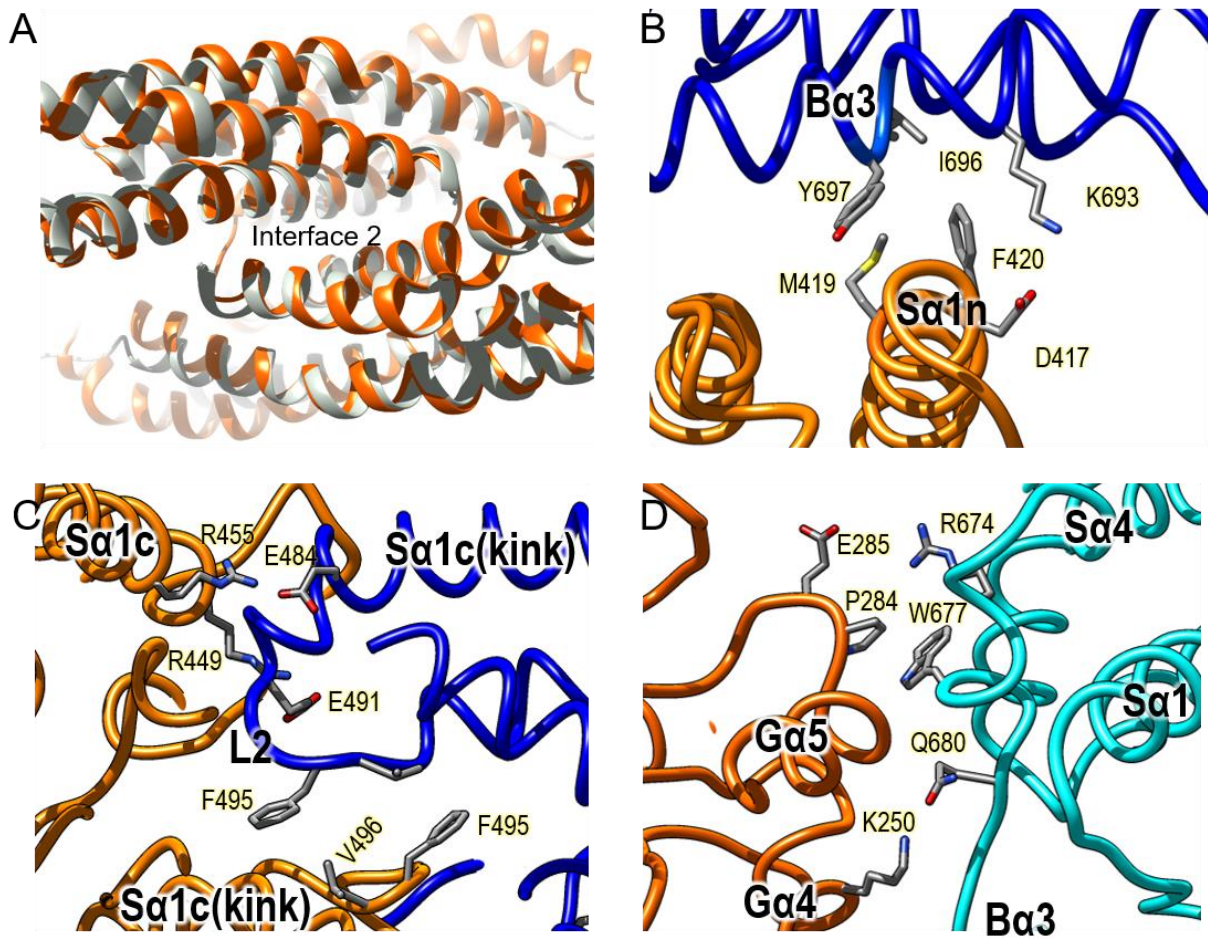


fig. S9. Enlarged views of the intermolecular interfaces in the MxB assembly. (A) Overlay of the MxB crystal dimer (grey) and the cryoEM dimer (orange) at the dimer interface, Interface 2. (B to D) Detailed view of the Interface 1 (B), Interface 3 (C) and Interface 4 (D). Specific residues at the interfaces are labeled.

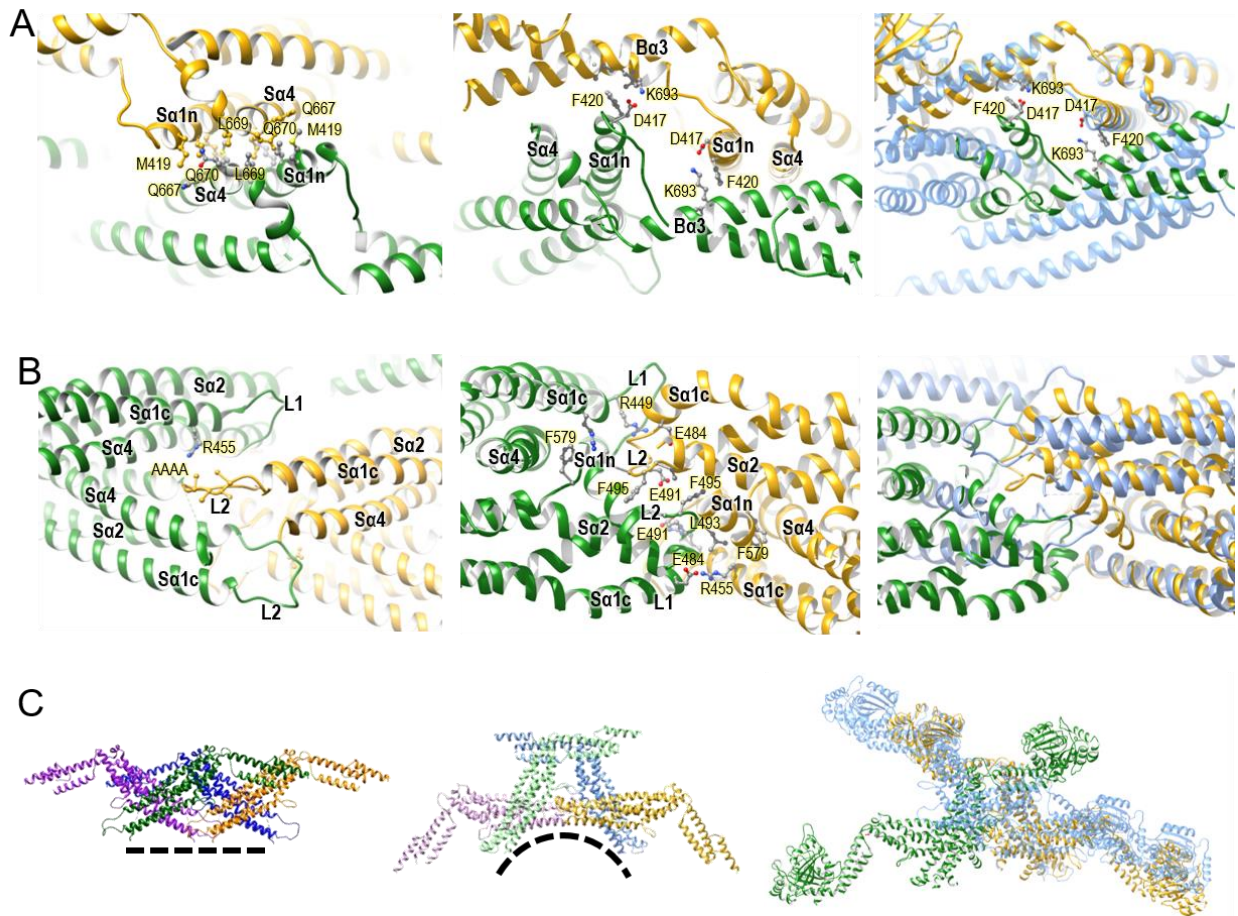


fig. S10. Comparison of interfaces between cryoEM and crystal structures. (A) Putative interface 1 at crystal contacts (4WHJ) (left), Interface 1 in the cryoEM assembly (middle) and overlay of the two interfaces (cryoEM gold/green, 4WHJ, light blue). The intermolecular interactions are entirely different. (B) Hypothetical Interface 3 (26) (no interaction) in the crystal structure (4WHJ) (left), extensive interactions at Interface 3 in the cryoEM assembly (middle), and overlay of the interfaces (cryoEM gold/green, 4WHJ, light blue). Amino acids involved in the interfaces are shown. Alpha helices and loops are labeled. (C) Connection of two adjacent MxB dimers in linear crystal arrays (left), cryoEM curved assembly (middle) with each monomer colored individually, excluding G domains for clarity, and overlay of crystal (light blue) and cryoEM (gold/green) (right), showing completely different dimer/dimer organization.

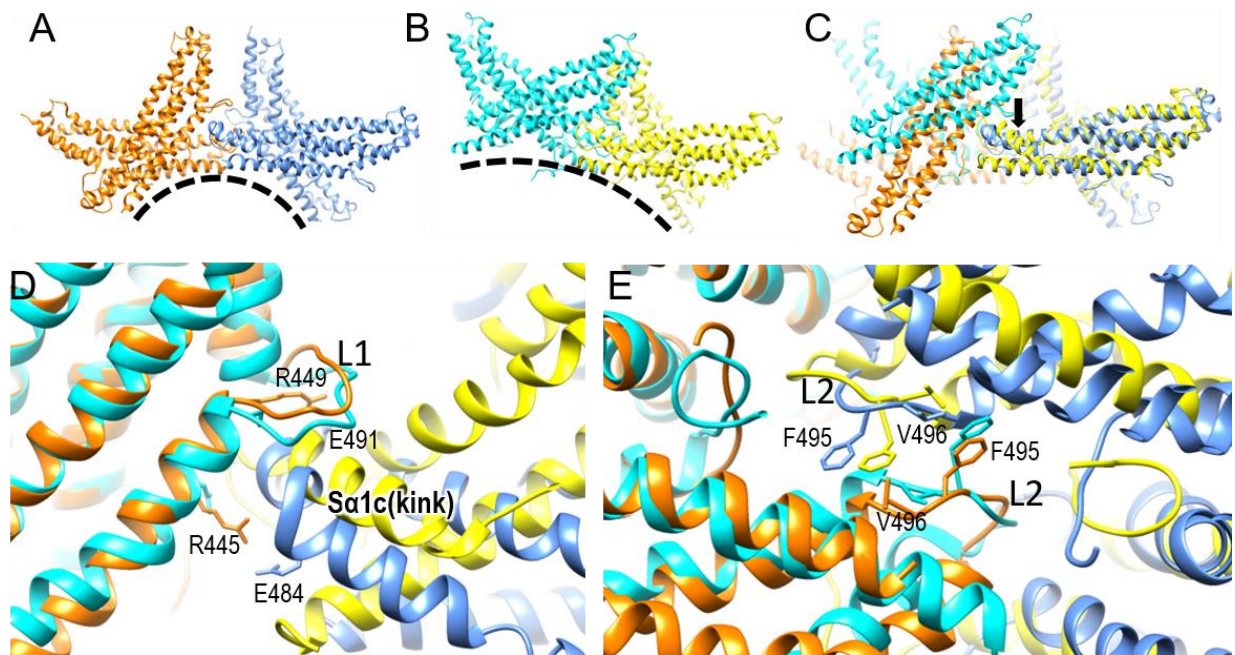


fig. S11. Comparison of L1 and L2 contacts of MxB and dynamin 3. (A to B) Tetramers of MxB (A, orange and blue) and dynamin 3 (5A3F, B, cyan and yellow) show different degrees of curvature (black dashed line). Only the stalk domains are shown for clarity. The dimers are individually colored. (C) The stalk tetramers were superposed using the blue (MxB) and yellow (dynamin 3) dimer pairs, which aligned with RMSD of 1.146 Å. The orange and cyan dimers clearly do not overlay well. (D) Superposition of MxB and dynamin 3 at Interface 3 at L1. Residues from MxB are shown. Differences between MxB and dynamin 3 are observed. (E) Superposition of MxB and dynamin 3 at Interface 3 residues in L2, wherein a similar interface is seen between MxB and dynamin 3. Residues from both MxB and dynamin 3 are shown.

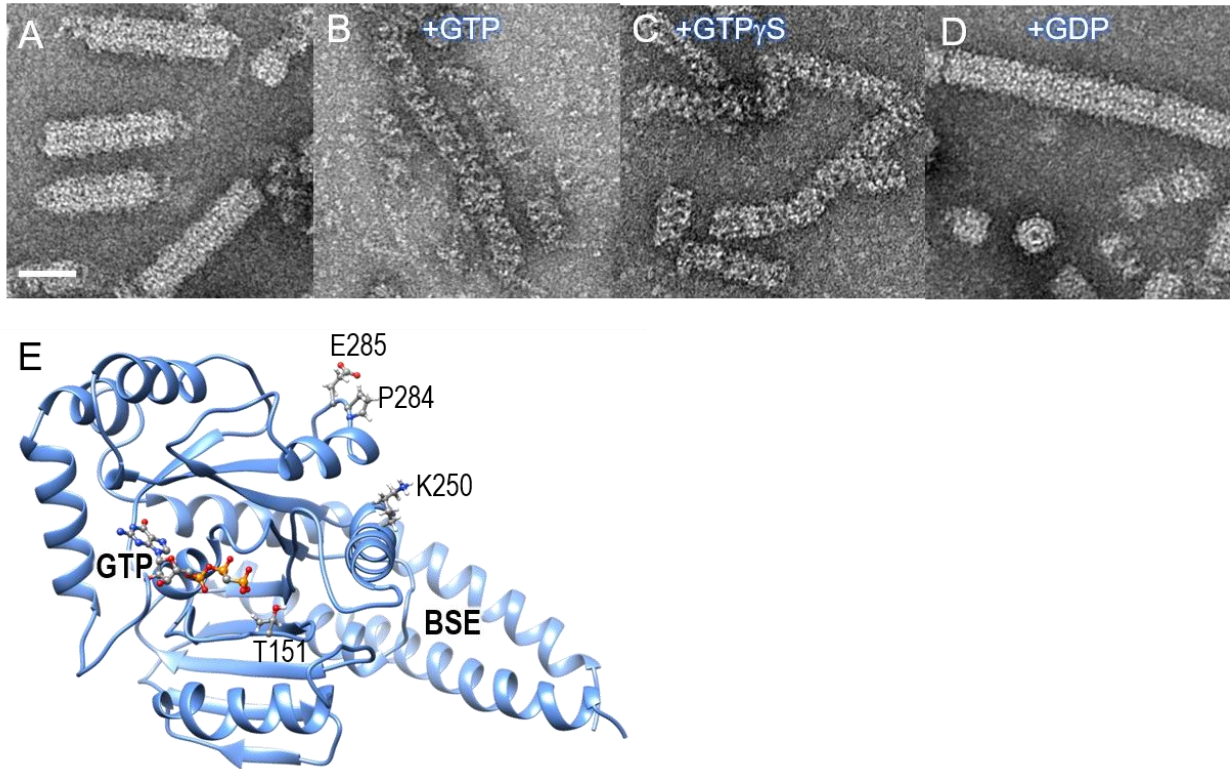


fig. S12. Interface 4 mutations relative to GTP-binding site. (A to D) MBP-MxB-T151A has been shown to bind GTP γ S (28) but is unable to hydrolyze GTP. MBP-MxB-T151A self-assembled into ordered tubular structures at 150 mM NaCl (A) or in the presence of GDP (D), loosened tubes in the presence of GTP (B) or GTP γ S. Scale bar, 50 nm. (E) GTPase domain of MxB is shown, with residues at Interface 4 (P284, E285 and K250) located at the opposite side of GTP binding site (T151) labeled.

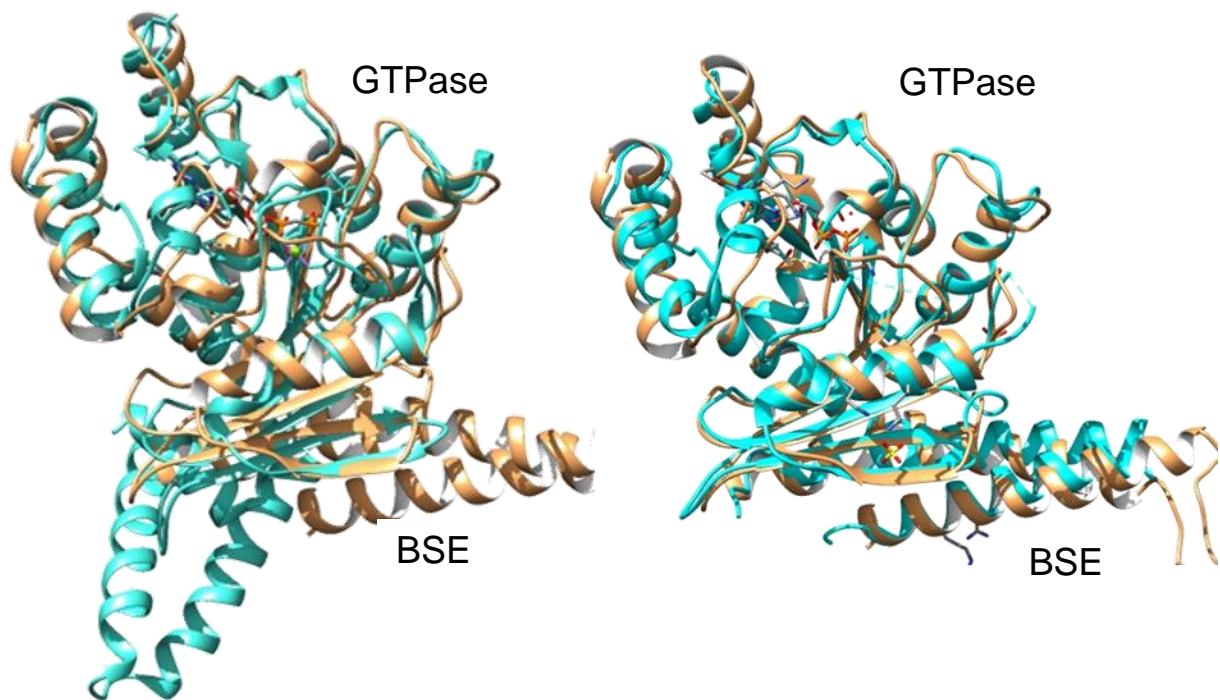


fig. S13. Comparison of MxB and MxA GTPase-BSE domains. MxB GTPase-BSE domains (orange) are overlaid with the corresponding domains in MxA (cyan) in GMP-PCP bound “open” state (4P4S, left) and MxA in GDP-bound “closed” state (4P4T, right).